



MODELING OF ELECTROMAGNETIC DEVICES FOR MEASURING ASYMMETRIC REACTIVE POWER CURRENT PROCESSES IN A HYBRID POWER SUPPLY SYSTEM NETWORK

A. B. Abubakirov

Nukus Mining Institute at Navoi State University of Mining and Technologies,
Nukus, Uzbekistan, aziz1306@mail.ru

Abstract:

This article presents the modeling of reactive power currents in hybrid energy source electrical supply systems using primary asymmetric processes, employing collected and distributed parameter graph models as well as analytical expressions to ensure high accuracy for electromagnetic devices.

Keywords: Reactive power, graph model, modeling, electromagnetic device, electrical supply, analytical expression.

1. INTRODUCTION:

Worldwide, significant attention is being given to the advancement of electromagnetic conversion devices, components, and systems, as well as structures that ensure standardized maintenance and precisely defined quality of reactive energy and power in three-phase current networks within power supply systems using hybrid energy sources.

In developed countries, a key issue is the development of primary electromagnetic converter structures that provide high-accuracy measurement and remote monitoring of three-phase reactive power currents in electrical networks with hybrid energy sources. Of particular importance is the creation, investigation, and practical implementation of new types of these converter devices and the principles behind their design [1].



Currently, extensive scientific research is being conducted on primary conversion devices for measuring and remotely monitoring three-phase reactive power currents in networks with hybrid energy sources. These studies aim to advance the principles of design and application of such devices, as well as to address energy supply challenges through the use of primary conversion equipment for measuring and remotely monitoring reactive power quality indicators in electricity, in pursuit of effective, high-quality, and reliable solutions.

An analysis has shown that the comprehensive application of modern digital technologies for converting primary reactive currents of three-phase electrical networks with hybrid energy sources into secondary signals, as well as the modeling, algorithmization, and analysis of processes in remote measurement and control devices, has not been sufficiently explored. Moreover, issues such as the feasibility of current transmission in electrical networks with hybrid energy sources, structural and parametric studies of current measurement and remote control devices (which represent key electrical quantities), and the development of modern principles for constructing devices that convert three-phase reactive power currents and their implementation in practice, remain insufficiently investigated [2].

2. MATERIALS AND METHODS:

Principles for Constructing Reactive Current Converter Devices for Three-Phase Networks with Isolated Neutrals. The device provides closed magnetic flux loops generated by three-phase reactive power currents. It features extended functional capabilities for adjusting the magnitude and characteristics of unbalanced three-phase currents and is equipped with a magnetic core that includes an adjustable air gap. The construction principles of three-phase reactive power current converters are shown in Figure 1.

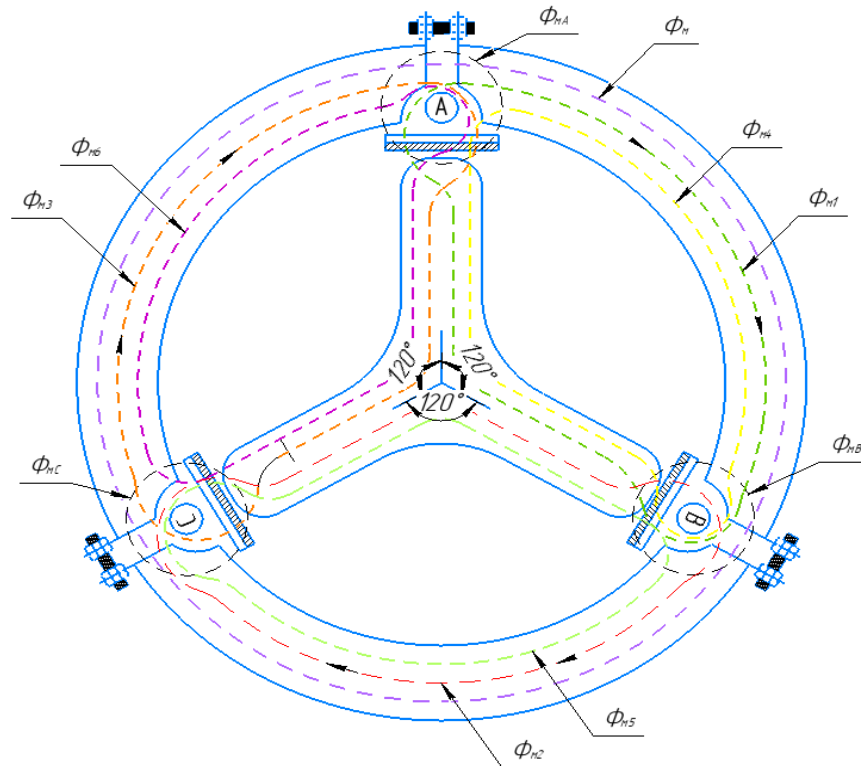


Figure 1. Principles of constructing three-phase reactive power current converters with isolated neutral

Here: $\Phi_{\mu A}$, $\Phi_{\mu B}$, $\Phi_{\mu C}$ – the main magnetic fluxes generated by the currents of phases A, B and C of the electrical network, which pass through the corresponding sensing elements; $\Phi_{\mu 1}$, $\Phi_{\mu 2}$, $\Phi_{\mu 3}$, $\Phi_{\mu 4}$, $\Phi_{\mu 5}$, $\Phi_{\mu 6}$ – magnetic fluxes generated by the currents between phases, which are not primary for the sensing elements; δ – the air gap through which the magnetic fluxes pass in the magnetic core.

Research Model. In converting the three-phase primary currents flowing from electrical power supply networks (EPSNs) into secondary voltage or signal form, a signal conversion principle is applied. In particular, when using three simple measuring windings or flat measuring windings in Electromagnetic Devices for Measuring Asymmetric Reactive Power Currents (EDMARPC), the primary currents, the conversion circuit or structure, its geometric shape and dimensions, as well as the applied signal conversion principle based on physical and technical effects, are studied according to the following algorithms [3,4]:

a) A graph model has been developed for generating the secondary voltage of a single-phase, single-sensing-element device with lumped parameters in a three-phase reactive power current electrical network with an isolated neutral connected to a reactive power source of the electrical power supply network (EPSN) (see Figure 1).

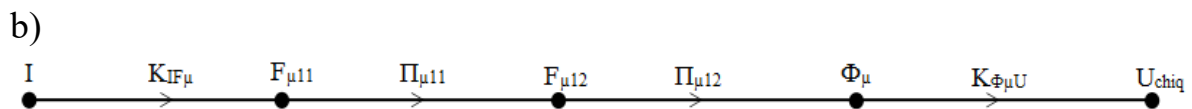


Figure 2. Lumped-parameter graph model for generating the secondary voltage of a three-phase current converter device with isolated neutral

An analytical expression (2) is formulated based on the lumped-parameter graph model for generating the output voltage of a single-phase, single-sensing-element Electromagnetic Device for Measuring Asymmetric Reactive Power Currents (EDMARPC) in an electrical network with an isolated neutral connected to a reactive power source of the electrical power supply network (EPSN) [2, 5-9]:

$$U_{chiq} = W_{IU_{chiq}} (IU_{chiq}) I = K_{IF\mu} \Pi_{\mu} K_{\Phi_{\mu}U_{chiq}} I = (4.44fw_2w_1/R_{\mu}) I \quad (1)$$

Here: Transfer function of converting the primary current I into the secondary voltage U_{out} through the conversion element $W_{IU_{chiq}} (IU_{chiq}) = K_{IF\mu} \Pi_{\mu} K_{\Phi_{\mu}U_{chiq}}$;
Inter-circuit conversion coefficient from primary current to magnetic flux $K_{IF\mu}$;
Inter-circuit conversion coefficient from magnetic flux to voltage $K_{\Phi_{\mu}U_{chiq}}$;

I – primary current of the electrical network;

f – frequency of the electrical network current;

w_2, w_1 – number of turns of the primary and secondary windings of the electromagnetic device for measuring asymmetric reactive power currents (EDMARPC);

$\Pi_{\mu} = R_{\mu} - \frac{\rho L}{F}$ – resistance of the signal conversion element (magnetic resistance);

ρ – relative resistivity of the magnetic core material;

L – length of the magnetic flux path;

F – geometric cross-sectional area of the magnetic core.

c) A graph model of the secondary voltage of the EDMARPC with three sensitive elements of a distributed-parameter three-phase reactive power current electric network with an isolated neutral connected to a reactive power source of EPSN has been formed (Figure 3).

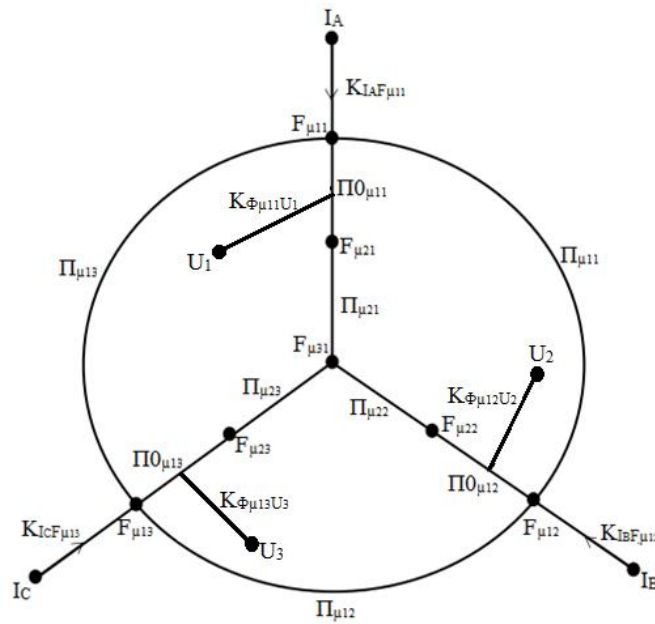


Figure 3. Graph model of the secondary voltage formation of a neutral-isolated three-phase current converter device with distributed parameters. Based on the graph model of the distributed-parameter three-phase EDMARPC with three sensitive elements, the analytical expression for generating the electromotive forces (EMFs) through the currents takes the following form (2) [8, 9]:

$$\left\{ \begin{array}{l} \frac{F_{\mu 11}-F_{\mu 12}}{\Pi_{\mu 11}} + \frac{F_{\mu 11}-F_{\mu 21}}{\Pi_{\mu 11}} + \frac{F_{\mu 11}-F_{\mu 13}}{\Pi_{\mu 13}} = K_{I_A F_{\mu 11}} I_A; \\ \frac{F_{\mu 21}-F_{\mu 11}}{\Pi_{\mu 11}} + \frac{F_{\mu 21}-F_{\mu 31}}{\Pi_{\mu 21}} = 0; \\ \frac{F_{\mu 12}-F_{\mu 11}}{\Pi_{\mu 11}} + \frac{F_{\mu 12}-F_{\mu 22}}{\Pi_{\mu 12}} + \frac{F_{\mu 12}-F_{\mu 13}}{\Pi_{\mu 12}} = K_{I_B F_{\mu 12}} I_B \\ \frac{F_{\mu 22}-F_{\mu 12}}{\Pi_{\mu 12}} + \frac{F_{\mu 22}-F_{\mu 31}}{\Pi_{\mu 22}} = 0; \\ \frac{F_{\mu 13}-F_{\mu 12}}{\Pi_{\mu 12}} + \frac{F_{\mu 13}-F_{\mu 22}}{\Pi_{\mu 13}} + \frac{F_{\mu 13}-F_{\mu 11}}{\Pi_{\mu 13}} = K_{I_C F_{\mu 13}} I_C \\ \frac{F_{\mu 23}-F_{\mu 13}}{\Pi_{\mu 13}} + \frac{F_{\mu 23}-F_{\mu 31}}{\Pi_{\mu 23}} = 0; \\ \frac{F_{\mu 31}-F_{\mu 21}}{\Pi_{\mu 21}} + \frac{F_{\mu 31}-F_{\mu 22}}{\Pi_{\mu 22}} + \frac{F_{\mu 31}-F_{\mu 23}}{\Pi_{\mu 23}} = 0. \end{array} \right. \quad (2)$$



The coefficients (w_a, w_b, w_c) depend on the number of turns of the sensitive elements' windings — $K_{I_A F_{\mu 11}}, K_{I_B F_{\mu 12}}, K_{I_C F_{\mu 13}}$; the primary currents — I_A, I_B, I_C ; the magnetic parameters of the magnetic core (rod) and air gap resistances — $\Pi_{ij}, \Pi O_{\mu ij}$; the electromotive forces (EMFs) in the device's magnetic core (rod) — $F_{\mu i, j}$.

From the resulting system of seven equations with unknowns, the distribution of the unknown EMFs in the magnetic conversion section is determined according to the magnetic parameters, and the values of the EMFs define the quantities of the transfer functions.

The analytical expressions of the relationships in the conversion process between the primary electric currents — I_A, I_B, I_C , the EMFs — $F_{\mu 11}, F_{\mu 12}, F_{\mu 13}$ the magnetic fluxes — $\Phi_{\mu 11}, \Phi_{\mu 12}, \Phi_{\mu 13}$ and the secondary output voltages — U_1, U_2, U_3 are formulated in forms (3), (4), and (5).

$$U_1 = K_{\Phi_{\mu 11} U_1} \Phi_{\mu 11}; \quad (3)$$

$$\Phi_{\mu 11} = \frac{F_{\mu 11} - F_{\mu 21}}{\Pi O_{\mu 11}};$$

$$F_{\mu 11} = K_{I_A F_{\mu 11}} I_A.$$

$$U_2 = K_{\Phi_{\mu 12} U_2} \Phi_{\mu 12}; \quad (4)$$

$$\Phi_{\mu 12} = \frac{F_{\mu 12} - F_{\mu 22}}{\Pi O_{\mu 12}};$$

$$F_{\mu 12} = K_{I_B F_{\mu 12}} I_B.$$

$$U_3 = K_{\Phi_{\mu 13} U_3} \Phi_{\mu 13}; \quad (5)$$

$$\Phi_{\mu 13} = \frac{F_{\mu 13} - F_{\mu 23}}{\Pi O_{\mu 13}};$$

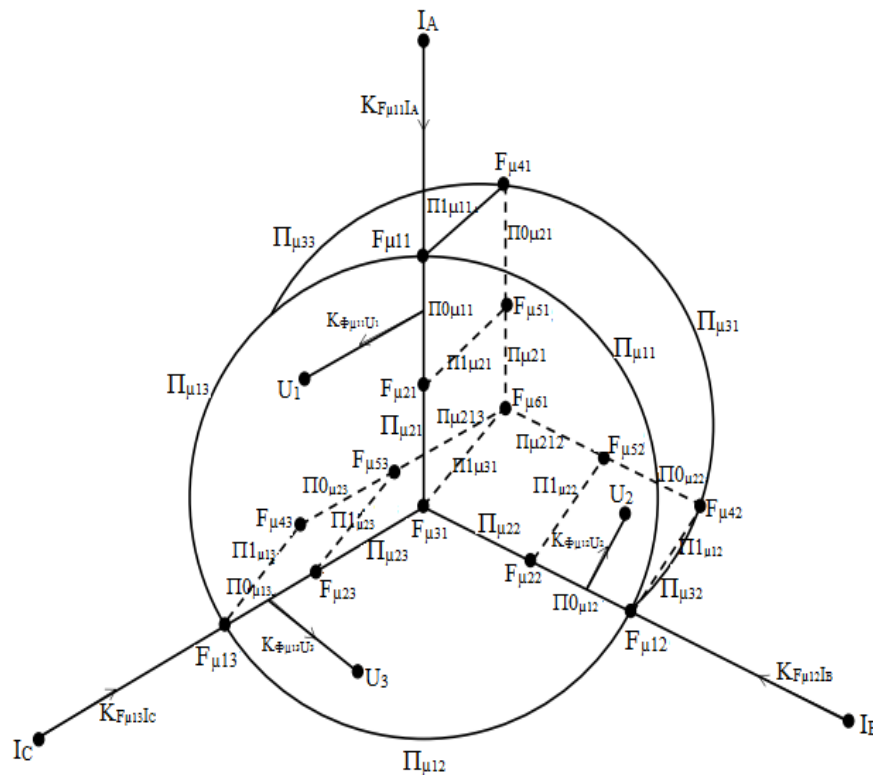
$$F_{\mu 13} = K_{I_C F_{\mu 13}} I_C.$$

Using the above expressions, the secondary voltages can be obtained through the electromotive forces (EMFs) generated by the magnetic fluxes as shown in (6), (7), and (8).

$$U_1 = K_{\Phi_{\mu 11} U_1} \left(\frac{K_{I_A F_{\mu 11}}}{\Pi O_{\mu 11}} I_A - \frac{F_{\mu 21}}{\Pi O_{\mu 11}} \right); \quad (6)$$

$$U_2 = K_{\Phi_{\mu 12} U_2} \left(\frac{K_{I_B F_{\mu 12}}}{\Pi O_{\mu 12}} I_B - \frac{F_{\mu 22}}{\Pi O_{\mu 12}} \right); \quad (7)$$

d) A graph model for generating the secondary voltage of a volumetric distributed-parameter three-phase device with three sensitive elements connected to a reactive power source in a HPS-based neutral-isolated three-phase electric network has been developed (Figure 4).



Based on the graph model of the volumetric distributed-parameter three-phase EDMARPC with three sensitive elements, the analytical expression for generating the electromotive forces (EMFs) through the currents takes the form of equation (9) [6]:

$$\left\{ \begin{array}{l} \frac{F_{\mu 11}-F_{\mu 12}}{\Pi_{\mu 11}} + \frac{F_{\mu 11}-F_{\mu 121}}{\Pi_{0 \mu 11}} + \frac{F_{\mu 11}-F_{\mu 13}}{\Pi_{\mu 13}} + \frac{F_{\mu 11}-F_{\mu 41}}{\Pi_{1 \mu 11}} = K_{I_A F_{\mu 11}} I_A; \\ \frac{F_{\mu 21}-F_{\mu 11}}{\Pi_{0 \mu 11}} + \frac{F_{\mu 21}-F_{\mu 31}}{\Pi_{\mu 21}} + \frac{F_{\mu 21}-F_{\mu 51}}{\Pi_{1 \mu 21}} = 0; \\ \frac{F_{\mu 12}-F_{\mu 11}}{\Pi_{\mu 11}} + \frac{F_{\mu 12}-F_{\mu 22}}{\Pi_{0 \mu 12}} + \frac{F_{\mu 12}-F_{\mu 13}}{\Pi_{\mu 12}} + \frac{F_{\mu 12}-F_{\mu 42}}{\Pi_{1 \mu 12}} = K_{I_B F_{\mu 12}} I_B; \\ \frac{F_{\mu 22}-F_{\mu 12}}{\Pi_{0 \mu 12}} + \frac{F_{\mu 22}-F_{\mu 31}}{\Pi_{\mu 22}} + \frac{F_{\mu 22}-F_{\mu 52}}{\Pi_{1 \mu 22}} = 0; \\ \frac{F_{\mu 13}-F_{\mu 12}}{\Pi_{\mu 12}} + \frac{F_{\mu 13}-F_{\mu 22}}{\Pi_{0 \mu 13}} + \frac{F_{\mu 13}-F_{\mu 11}}{\Pi_{\mu 13}} + \frac{F_{\mu 13}-F_{\mu 43}}{\Pi_{1 \mu 13}} = K_{I_C F_{\mu 13}} I_C; \\ \frac{F_{\mu 23}-F_{\mu 13}}{\Pi_{0 \mu 13}} + \frac{F_{\mu 28}-F_{\mu 13}}{\Pi_{\mu 23}} + \frac{F_{\mu 23}-F_{\mu 53}}{\Pi_{1 \mu 23}} = 0; \\ \frac{F_{\mu 31}-F_{\mu 21}}{\Pi_{\mu 21}} + \frac{F_{\mu 31}-F_{\mu 22}}{\Pi_{\mu 22}} + \frac{F_{\mu 31}-F_{\mu 23}}{\Pi_{\mu 23}} + \frac{F_{\mu 31}-F_{\mu 61}}{\Pi_{1 \mu 31}} = 0. \end{array} \right. \quad (9)$$

The analytical expressions of the relationships in the conversion process between the primary electric currents — I_A , I_B , I_C , the electromotive forces (EMFs) — $F_{\mu 11}$, $F_{\mu 12}$, $F_{\mu 13}$ the magnetic fluxes — $\Phi_{\mu 11}$, $\Phi_{\mu 12}$, $\Phi_{\mu 13}$ and the secondary output voltages — U_1 , U_2 , U_3 are formulated in forms (10), (11), and (12).

$$U_1 = K_{\Phi_{\mu 11} U_1} \Phi_{\mu 11}; \quad (10)$$

$$\Phi_{\mu 11} = \frac{F_{\mu 11}-F_{\mu 21}}{\Pi_{0 \mu 11}} + \frac{F_{\mu 11}-F_{\mu 41}}{\Pi_{1 \mu 11}};$$

$$F_{\mu 11} = K_{I_A F_{\mu 11}} I_A.$$

$$U_2 = K_{\Phi_{\mu 12} U_2} \Phi_{\mu 12}; \quad (11)$$

$$\Phi_{\mu 12} = \frac{F_{\mu 12}-F_{\mu 22}}{\Pi_{0 \mu 12}} + \frac{F_{\mu 12}-F_{\mu 42}}{\Pi_{1 \mu 12}};$$

$$F_{\mu 12} = K_{I_B F_{\mu 12}} I_B.$$

$$U_3 = K_{\Phi_{\mu 13} U_3} \Phi_{\mu 13}; \quad (12)$$

$$\Phi_{\mu 13} = \frac{F_{\mu 13}-F_{\mu 23}}{\Pi_{0 \mu 13}} + \frac{F_{\mu 13}-F_{\mu 43}}{\Pi_{1 \mu 13}};$$

$$F_{\mu 13} = K_{I_C F_{\mu 13}} I_C.$$

Using the above expressions, the secondary voltages can be obtained through the electromotive forces (EMFs) generated by the magnetic fluxes as shown in (13), (14), and (15).

$$U_1 = K_{\Phi_{\mu 11} U_1} \left(\frac{K_{I_A F_{\mu 11}}}{\Pi_{0 \mu 11}} I_A - \frac{F_{\mu 21}}{\Pi_{0 \mu 11}} - \frac{F_{\mu 41}}{\Pi_{1 \mu 11}} \right); \quad (13)$$

$$U_2 = K_{\Phi_{\mu 12}} U_2 \left(\frac{K_{I_A} F_{\mu 12}}{\Pi O_{\mu 12}} I_B - \frac{F_{\mu 22}}{\Pi O_{\mu 12}} - \frac{F_{\mu 42}}{\Pi 1_{\mu 12}} \right); \quad (14)$$

$$U_3 = K_{\Phi_{\mu 13}} U_3 \left(\frac{K_{I_C} F_{\mu 13}}{\Pi O_{\mu 13}} I_C - \frac{F_{\mu 23}}{\Pi O_{\mu 13}} - \frac{F_{\mu 43}}{\Pi 1_{\mu 13}} \right); \quad (15)$$

3. RESULTS AND DISCUSSION:

In the presented model, the primary variables are taken as I_A , I_B , I_C - primary currents (within the range of 1-131.5 amperes). W_A , W_B , W_C — number of turns of the input windings (1-3 turns), W_1 , W_2 , W_3 - number of turns of the output windings of the sensitive elements (1-9 turns).

Research was conducted based on the model by varying the winding range, and the theoretical and practical results were relatively compared with the output signals of classical current transformers (Figure 5).

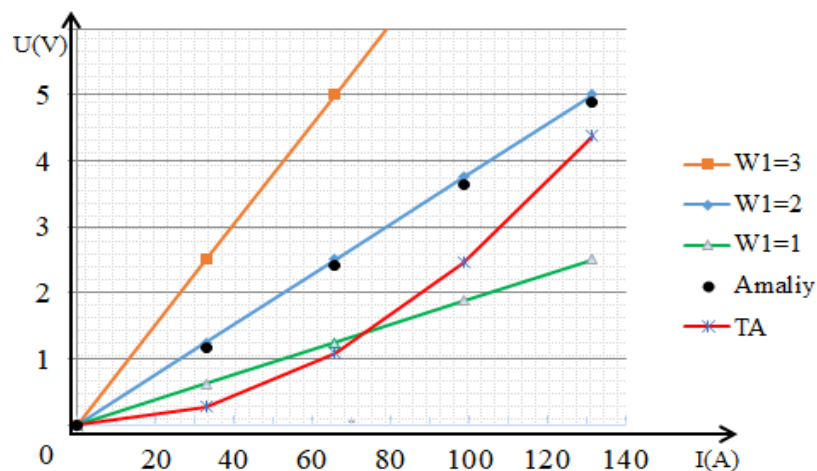


Figure 5. Relative static characteristic expressing the dependence of the secondary output signal of neutral-isolated three-phase current conductors on the reactive power primary currents $I = 131.5$ A in the electric network.

Here, W_1 — the dependence characteristic of the output voltage on the variation of current strength obtained from the lumped parameter model based on the change in the number of secondary windings turns (according to equation's 13, 14, 15 the variation of the output voltage corresponding to the current I_A). **TA** — the practical characteristic of classical current transformers.



The table of output voltage variation depending on the number of turns of the sensitive element windings when the input current is $I = 131.5$ A is as follows (Table 1):

Table 1 Variation of the output voltage depending on the number of turns of the sensitive element windings when the input current is $I = 131.5$ A.

Primary Currents – I [A]	Secondary Voltage Signals – U [V] (Theoretical)	Secondary Voltage Signals – U [V] (Practical)	Secondary Voltage Signals – U [V] (Classical Current Transformers)	Number of Sensitive Element Turns – W2
32,87	1,25	1,162	0,27	3
65,75	2,5	2,441	1,09	5
98,62	3,75	3,641	2,46	7
131,5	5	4,88	4,37	9

The comparison results show that the adequacy between the theoretical and practical measurement results of the output signal of the GEM-based reactive power current converter device in the electric network is **2.4%** for the neutral-isolated three-phase device. Moreover, compared to the practical results of classical current transformers, the neutral-isolated three-phase device shows an improvement of **10.4%**.

$$\delta_{NUF} = \frac{U_{nazariy} - U_{amaliy}}{U_{nazariy}} 100\% = \frac{5 - 4,88}{5} 100\% = 2,4 \%,$$

$$\delta_{NUF} = \frac{U_{amaliy} - U_{TA amaliy}}{U_{amaliy}} 100\% = \frac{4,88 - 4,37}{4,88} 100\% = 10,4 \, \%.$$

4. CONCLUSION:

1. In electromagnetic current-to-voltage converters, the method for calculating the values of the output voltages U_1 , U_2 , and U_3 generated in the sensitive elements - based on the criterion of uniform and orthogonal distribution of the magnetic flux crossing the surface of the converter's sensitive elements, as well as the values of the magnetomotive force and magnetic flux in the converter sections - has been developed using distributed parameter graph models.



2. The distributed parameter graph model of GEM-based three-phase reactive power current devices and their corresponding mathematical models have been proven to be adequate in representing the real linear output characteristics of the devices. For the neutral-isolated three-phase network, the conversion accuracy of the developed device was improved by **2.4%** compared to the lumped parameter model and by **10.4%** compared to the classical current transformer.

REFERENCES

1. Siddikov I.X., Abubakirov A.B., Kurbaniyazov T.U., Bekimbetov M.N., Uch fazali tokning nosimmetrikligini kuchlanishga o'tkazuvchi elektromagnitli o'zgartirgich // Patent RUz (UZ) № FAP 02157 U.S. 27.05. 2022 y.
2. Abubakirov A.B. Analysis of cloud computing of digital monitoring of nonlinear values and parameters of electric networks // Journal of Engineering and Technology (JET), ISSN(P):2250-2394; ISSN(E): Applied Vol. 12, Issue 2, Dec 2022, 35–44.
3. Azizjan Abubakirov, Timur Kurbaniyazov and Muratbay Bekimbetov. Analysis of three-phase asymmetrical currents in the secondary voltage of signal change sensors in the power supply system using graph models // E3S Web of Conferences 525, 03013 (2024), GEOTECH-2024, -T. №1.
4. Azizjan Abubakirov, Naurizbek Eshmuratov, Gulayim Esemuratova, and Muzaffar Nazarov. Electromagnetic converter of reactive power and monitoring of high-voltage induction motors // E3S Web of Conferences 525, 03016 (2024), GEOTECH-2024, -T. №1.
5. I.Kh.Siddikov, P.D.Chelyshkov, A.B.Abubakirov, N.M.Nazhimatdinov, R.Zh.Tanatarov. Structure of control sensors of multi-phase reactive power currents in power supply systems // Agribusiness, Environmental Engineering and Biotechnologies» IOP Conference Series: Earth and Environmental Science 839 (5), 052045. pp. 1-9. doi:10.1088/1755-1315/839/5/052045. (AGRITECH-V - 2021). Publication Year: 2021. <https://iopscience.iop.org/article/10.1088/1755-1315/839/5/052045/pdf>
6. A. Djalilov, O. Matchonov, A. Abubakirov, J. Abdunabiev, A. Saidov. System for measuring and analysis of vibration in electric motors of irrigation facilities // Agricultural Engineering and Green Infrastructure Solutions. IOP



Conference Series: Earth and Environmental Science, Volume 868, International Conference on Agricultural Engineering and Green Infrastructure Solutions (AEGIS 2021) 12th-14th May 2021, Tashkent, Uzbekistan. <https://iopscience.iop.org/article/10.1088/1755-1315/868/1/012032>

7. I.Siddikov, A.B.Abubakirov, R.Seytimbetov, Sh.Kuatova, Yu.Lezhnina. Analysis of current conversion primary sensors dynamic characteristics of a reactive power source with renewable energy sources into secondary voltage // Part 1. E3S Web of Conferences 281, 09028. CATPID-2021. Publication Year: 2021.
8. I.Kh.Siddikov, M.A.Anarbaev, A.A.Abdumalikov, A.B.Abubakirov, M.T.Maxsudov, I.M.Xonturaev. «Modelling of transducers of nonsymmetrical signals of electrical nets» // International Conference On Information Science And Communications Technologies Applications, Trends And Opportunities // Publication Year: 2019, Page(s): 1–6. <http://WWW.ICISCT2019.Org>
9. I.X.Siddikov, A.B.Abubakirov, A.J.Allanazarova, R.M.Tanatarov, Sh.B.Kuatova // Modeling the secondary strengthening process and the sensor of multiphase primary currents of reactive power of renewable electro energy supply // Solid State Technology, Volume: 63 Issue: 6, Publication Year: 2020, pp: 13143-13148.